一般社団法人　電子情報通信学会
THE INSTITUTE OF ELECTRONICS,
INFORMATION AND COMMUNICATION ENGINEERS

信学技報
IEICE Technical Report
RCS2017-135 (2017-07)

A Study on PAPR Reduction for MU-MIMO using Blind Selected Mapping

Amnart Boonkajay† and Fumiyuki Adachi‡

†‡Research Organization of Electrical Communication (ROEC), Tohoku University
2-1-1 Katahira, Aoba-ku, Sendai, Miyagi, 980-8577 Japan
E-mail: †amnart@riec.tohoku.ac.jp ‡adachi@ecei.tohoku.ac.jp

Abstract Peak-to-average power ratio (PAPR) of single-carrier (SC) waveform in multi-user multiple-input multiple-output (MU-MIMO) uplink transmission becomes higher than that of single-antenna transmission due to the use of transmit filtering. An antenna-wise selected mapping (SLM) can effectively lower the PAPR of MIMO uplink transmit signal waveform, but side-information transmission is mandatory. In this paper, we study an SLM without side-information transmission (called blind SLM) for SC-MU-MIMO uplink with MMSE-SVD which uses singular value decomposition (SVD) transmit filtering and minimum mean-square error (MMSE) receive filtering. To realize a simple data detection without side-information, we recommend that the phase rotation sequence multiplication should be applied to transmit data streams before applying the transmit filtering (called stream-wise SLM). Phase rotation sequence selection is done so as to minimize the maximum instantaneous PAPR associated with all transmit antennas. At the receiver, the phase rotation sequence estimation is done for each user's data streams after applying the receive filtering. Simulation results confirm that the stream-wise blind SLM for uplink MMSE-SVD can effectively reduce the PAPR of transmit waveforms, while there is no significant bit-error rate (BER) degradation although the data detection is carried out without side-information.

Keyword MU-MIMO, peak-to-average power ratio (PAPR), selected mapping (SLM)

1. Introduction

High peak-to-average power ratio (PAPR) signal remains a major problem in mobile communications since it degrades energy efficiency of battery-operated user equipment (UE) [1]. Single-carrier (SC) waveform is well-known as a low-PAPR waveform compared to orthogonal frequency division multiplexing (OFDM) waveform [2]. Broadband SC with multi-user multiple-input multiple-output (MU-MIMO) transmission [3] can significantly increase the spectrum efficiency by allowing multiple users to transmit multiple data streams over the same bandwidth. SC-MU-MIMO uplink with MMSE-SVD using singular-value decomposition (SVD) based transmit (Tx.) filtering and minimum mean-square error (MMSE) based receive (Rx.) filtering was introduced recently [4], where it can achieve better bit-error rate (BER) than zero-forcing (ZF) based Rx. filtering.

However, PAPR increases when the Tx. filtering are employed even in SC waveform [5], indicating that PAPR reduction techniques are also necessary for SC. Among various PAPR techniques, selected mapping (SLM) [6] is well-known as an efficient and simple PAPR reduction scheme. SLM selects the waveform having the lowest PAPR among many candidates generated by phase rotations. The SLM in [6] is originally for OFDM and requires side-information transmission. SLM without side-information (blind SLM) for SC has been proposed in [7], where its extensions for space-time block coded transmit diversity (STBC-TD) with and without Tx. frequency-domain equalization (Tx-FDE) were discussed in [8] and [9], respectively. However, blind SLM for uplink MMSE-SVD transmission has not been yet discussed.

There is a conventional SLM for OFDM-MIMO transmission employing phase rotation individually at each transmit antenna (antenna-wise SLM) [10], which achieves the same PAPR as single-antenna transmission. A suboptimal SLM which applies phase rotation directly to the transmit antenna emitting high-PAPR signal (called directed SLM) was proposed in [11] in order to reduce the computational complexity. The directed SLM without explicit side-information transmission was also studied in [12]. Although the SLM techniques in [10]-[12] are possible to apply to SC signals, they did not consider the use of Tx. filtering. More importantly, it is difficult to conduct signal detection without side-information in uplink MMSE-SVD when the SLMs in [10]-[12] are considered since the phase rotation estimation at the receiver needs to consider all possible Rx. filter coefficients.

In this paper, we introduce blind SLM for uplink MMSE-SVD, in which the phase rotation is multiplied to data streams prior to Tx. filtering (called stream-wise SLM). By using the above approach, phase rotation estimation can be employed independently for each user's data streams after Rx. filtering. No major changes on Tx. and Rx. filters implementation is required. Uplink MMSE-SVD (i.e. multiple UEs to single base station (BS)) using SVD Tx. filter and MMSE Rx. filter is considered in this paper. Two phase rotation methods can be considered when SC waveform is used, which are frequency-domain SLM (FD-SLM, i.e. phase rotation is applied to frequency components) and time-domain SLM (TD-SLM, i.e. phase

rotation is applied to data-modulated symbols). Performance evaluation of the stream-wise blind SLM for uplink MMSE-SVD is carried out by computer simulation and in aspects of PAPR and BER, where it is shown that the blind SLM can achieves low-PAPR transmission without degrading BER. In addition, computational complexity of the transceivers with SLM is also discussed.

2. Uplink MMSE-SVD transmission

SC uplink MMSE-SVD transmission system model is illustrated by Fig. 1. U UEs, each equipped with N_t Tx. antennas, simultaneously transmit multiple data streams to a single BS which has N_r Rx. antennas. We assume that each UE sends $G=N_t$ data streams and adaptive rank/modulation control (ARMC) [5] is not considered. The UE employs SVD-based Tx. filtering with joint Tx/Rx MMSE power allocation under an assumption that there is no channel state information (CSI) sharing among UEs, while the BS employs MMSE-based filtering generated based on full CSI knowledge [4]. Note that blind SLM is still not described in this section.

2.1. Transmit signals representation

At the u-th UE, information sequence is data-modulated into G streams of N_c-length block $\{\mathbf{d}_u(n);\ n=0\sim N_c-1\}$ with $\mathbf{d}_u(n)=[d_{u,0}(n),\ldots,d_{u,g}(n),\ldots,\ d_{u,G-1}(n)]^T$. Each stream is transformed into frequency-domain components block by discrete Fourier transform (DFT), yielding the frequency-domain components block $\{\mathbf{D}_u(k);\ k=0\sim N_c-1\}$ with $\mathbf{D}_u(k)=[D_{u,0}(k),\ldots,D_{u,g}(k),\ldots,\ D_{u,G-1}(k)]^T$ as

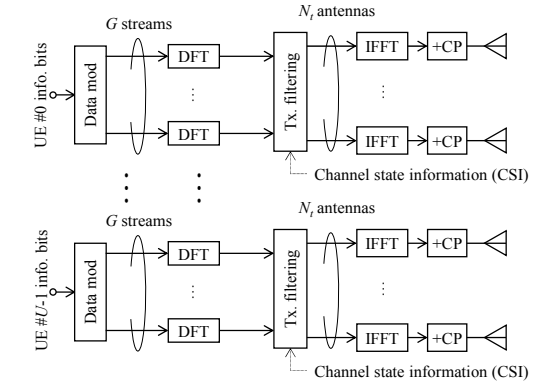

(a) Transmitters (UEs)

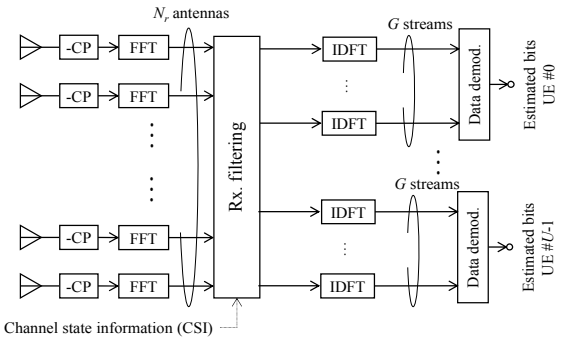

(b) Receiver (BS)

Fig. 1 SC uplink MMSE-SVD system model.

$$D_{u,g}(k)=\frac{1}{\sqrt{N_c}}\sum_{n=0}^{N_c-1}d_{u,g}(n)\exp(-j2\pi\frac{kn}{N_c}). \tag{1}$$

The frequency-domain component vector at the k-th subcarrier, $\mathbf{D}_u(k)$, is then multiplied by an $N_t\times G$ Tx. filtering matrix $\mathbf{W}_{T,u}(k)$, obtaining the frequency-domain uplink signal transmitted from N_t antennas of the u-th UE, $\mathbf{S}_u(k)=[S_{u,0}(k),\ldots,S_{u,n_t}(k),\ldots,S_{u,N_t-1}(k)]^T$, as

$$\mathbf{S}_u(k)=\sqrt{\frac{2E_s}{T_s}}\mathbf{W}_{T,u}(k)\mathbf{D}_u(k), \tag{2}$$

where E_s and T_s are symbol energy and symbol duration, respectively. $\mathbf{W}_{T,u}(k)$ is described in [4] and is given by

$$\mathbf{W}_{T,u}(k)=\mathbf{V}_u(k)\mathbf{P}_u^{1/2}(k), \tag{3}$$

where $\mathbf{V}_u(k)$ is an $N_t\times N_t$ unitary matrix whose columns consisting of right singular vector of an $N_r\times N_t$ channel matrix between the u-th UE and the BS, $\mathbf{H}_u(k)$, which is

$$\mathbf{H}_u(k)=\mathbf{U}_u(k)\mathbf{\Lambda}_u^{1/2}(k)\mathbf{V}_u^H(k). \tag{4}$$

Note that $\mathbf{A}^H$ represents Hermitian transpose of $\mathbf{A}$. $\mathbf{\Lambda}_u^{1/2}(k)$ is a $G\times G$ matrix whose the g-th diagonal element $\Lambda_{u,g}^{1/2}(k)$, $g=0\sim G-1$, contains an eigenvalue of the g-th eigenmode. $\mathbf{P}_u(k)$ is a $G\times G$ diagonal matrix representing MMSE power allocation, whose the g-th diagonal element is given by

$$P_{u,g}(k)=\max\left(\frac{1}{\sqrt{\mu_u}}\frac{1}{\sqrt{\frac{E_s}{N_0}\Lambda_{u,g}(k)}}-\frac{1}{\frac{E_s}{N_0}\Lambda_{u,g}(k)},0\right). \tag{5}$$

Note that μ_u is chosen for satisfying the power constraint and N_0 represents one-sided noise power spectrum density.

The frequency-domain signals $\{\mathbf{S}_u(k);\ k=0\sim N_c-1\}$ is transformed back into time domain by N_c-point inverse DFT (IDFT), yielding the time-domain blocks to be transmitted through N_t antennas $\{\mathbf{s}_u(n);\ n=0\sim N_c-1\}$ with $\mathbf{s}_u(n)=[s_{u,0}(n),\ldots,s_{u,n_t}(n),\ldots,s_{u,N_t-1}(n)]^T$ as

$$s_{u,n_t}(n)=\frac{1}{\sqrt{N_c}}\sum_{k=0}^{N_c-1}S_{u,n_t}(k)\exp(j2\pi\frac{kn}{N_c}). \tag{6}$$

Finally, the last N_g samples of transmit block are copied as a cyclic prefix (CP) and inserted into the guard interval (GI), then a CP-inserted signal block of N_g+N_c samples is transmitted from each antenna.

2.2. Received signals representation

At the BS, the CP-removed received signal blocks through N_r antennas are transformed into frequency domain by N_c-point DFT. The frequency-domain received signal vector at the k-th subcarrier, $\mathbf{R}(k)$, is expressed by

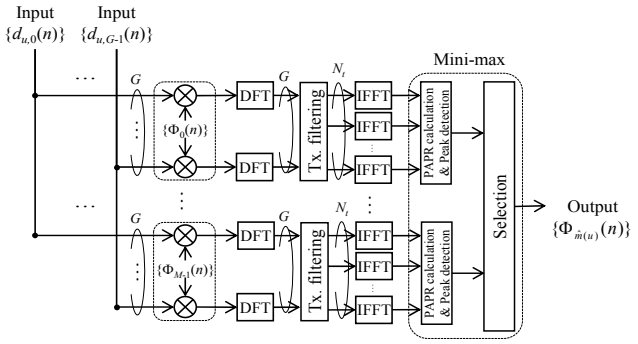

(a) Stream-wise TD-SLM algorithm

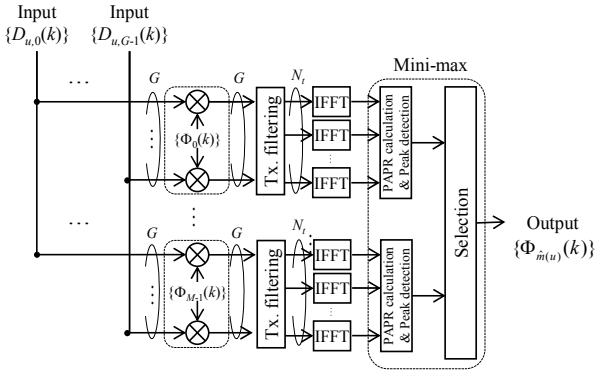

(b) Stream-wise FD-SLM algorithm

Fig. 2 Phase rotation sequence selection in stream-wise SLM.

$$\mathbf{R}(k)=\sum_{u=0}^{U-1}\mathbf{H}_u(k)\mathbf{S}_u(k)+\mathbf{Z}(k)$$
$$=\sqrt{\frac{2E_s}{T_s}}\left(\mathbf{H}_0(k)\mathbf{W}_{T,0}(k)...\mathbf{H}_{U-1}(k)\mathbf{W}_{T,U-1}(k)\right)\begin{bmatrix}\mathbf{D}_0(k)\\ \vdots \\ \mathbf{D}_{U-1}(k)\end{bmatrix}+\mathbf{Z}(k), \quad (7)$$

where $\mathbf{Z}(k)$ is an $N_r\times 1$ additive white Gaussian noise (AWGN) vector whose element has zero-mean and variance of $2N_0/T_s$. The frequency-domain output blocks $\{\hat{\mathbf{D}}(k);\ k=0\sim N_c-1\}$ with $\hat{\mathbf{D}}(k)=[\hat{\mathbf{D}}_0(k),...,\hat{\mathbf{D}}_u(k),...,\hat{\mathbf{D}}_{U-1}(k)]^T$ and $\hat{\mathbf{D}}_u(k)=[\hat{D}_0(k),...,\hat{D}_g(k),...,\hat{D}_{G-1}(k)]^T$ are obtained by applying MMSE filtering, i.e. $\hat{\mathbf{D}}(k)=\mathbf{W}_R(k)\mathbf{R}(k)$, where $\mathbf{W}_R(k)$ is a $G\times N_r$ matrix and is given by

$$\mathbf{W}_R(k)=\left(\mathbf{H}(k)\mathbf{W}_T(k)\right)^H\left(\left(\mathbf{H}(k)\mathbf{W}_T(k)\right)\left(\mathbf{H}(k)\mathbf{W}_T(k)\right)^H+\left(\frac{E_s}{N_0}\right)^{-1}\right)^{-1}, \quad (8)$$

where $\mathbf{H}(k)=[\mathbf{H}_0(k),\ldots,\mathbf{H}_u(k),\ldots,\mathbf{H}_{U-1}(k)]$ is the uplink channel between U UEs and the BS. $\mathbf{W}_T(k)$ is defined as $\mathbf{W}_T(k)=diag\{\mathbf{W}_{T,0}(k),\ldots,\mathbf{W}_{T,u}(k),\ldots,\mathbf{W}_{T,U-1}(k)\}$. Finally, the frequency-domain blocks $\{\hat{\mathbf{D}}(k)\}$ are transformed back into time domain by N_c-point IDFT, yielding the time-domain received blocks before data de-modulation $\{\hat{\mathbf{d}}(n);\ n=0\sim N_c-1\}$, with $\hat{\mathbf{d}}(n)=[\hat{\mathbf{d}}_0(n),...,\hat{\mathbf{d}}_u(n),...,\hat{\mathbf{d}}_{U-1}(n)]^T$ and $\hat{\mathbf{d}}_u(n)=[\hat{d}_0(n),...,\hat{d}_g(n),...,\hat{d}_{G-1}(n)]^T$.

3. Blind SLM algorithm

Blind SLM algorithm is described in details in this section. Assuming that an N_c-length time-domain transmit signal is $\{s(n);\ n=0\sim N_c-1\}$, PAPR can be calculated over a V-times oversampled block, which is defined by

$$\mathrm{PAPR}(\{s(n)\})=\frac{\max\{|s(n)|^2, n=0,\frac{1}{V},\frac{2}{V},...,N_c-1\}}{\frac{1}{N_c}\sum_{n=0}^{N_c-1}|s(n)|^2}. \quad (9)$$

3.1. Phase rotation sequence selection

The SLM for MIMO can achieve the same PAPR as that of single-antenna transmission if the phase rotation multiplication is carried out individually at each Tx. antenna (i.e. antenna-wise SLM [10]). However, the data detection without side-information in the antenna-wise SLM is difficult. Alternatively, we introduce stream-wise SLM for uplink MMSE-SVD filtering. Since the phase rotation sequence multiplication is done prior to Tx. filtering (i.e. phase rotation and filtering are carried out independently), there is no major changes on filter coefficients and hence, phase rotation sequence estimation becomes similar to that of single-antenna blind SLM [7].

Here, a codebook containing M different unit-magnitude sequences $\{\Phi_m(n);\ n=0\sim N_c-1,\ m=0\sim M-1\}$ is generated randomly as $\Phi_m(n)\in\{e^{j0},e^{j(2\pi/3)},e^{j(4\pi/3)}\}$, except the first pattern is defined as $\{\Phi_0(n)=e^{j0};\ n=0\sim N_c-1\}$ [7-9]. The stream-wise blind SLM for uplink MMSE-SVD can be categorized into 2 approaches.

(a) Stream-wise time-domain SLM (TD-SLM)

Stream-wise TD-SLM can be depicted by Fig. 2(a), where the phase rotation is applied to the time-domain data streams $\{\mathbf{d}_u(n);n=0\sim N_c-1\}$. The phase-rotated data streams corresponding to the m-th phase rotation sequence is $\{\mathbf{d}_u^m(n);n=0\sim N_c-1\}$, where $\mathbf{d}_u^m(n)$ is expressed by

$$\mathbf{d}_u^m(n)=[\Phi_m(n)d_{u,0}(n),...,\Phi_m(n)d_{u,g}(n),...,\Phi_m(n)d_{u,G-1}(n)]^T. \quad (10)$$

The data streams in (10) are then passed through transmit signal processing described in (1)-(6), yielding the time-domain waveforms $\{\mathbf{s}_u^m(n);\ n=0\sim N_c-1\}$ where $\mathbf{s}_u^m(n)=[s_{u,0}^m(n),...,s_{u,n_t}^m(n),...,s_{u,N_t-1}^m(n)]^T$. PAPR calculation is carried out at each Tx. antenna, where the transmit block at the n_t-th antenna is defined as $\{s_{u,n_t}^m(n);\ n=0\sim N_c-1\}$.

Meanwhile, it is difficult to minimize the PAPR of each Tx. antenna at the same time when using the stream-wise SLM due to matrix multiplication operations (This is similar to the SLM for STBC-TD with Tx-FDE [8]). Instead, the phase rotation sequence selection is done based on the worst case, i.e. minimizing the maximum instantaneous PAPR of all N_t antennas. The selected phase rotation sequence for the u-th user $\{\Phi_{\hat{m}(u)}(n);\ n=0\sim N_c-1\}$, with the corresponding index $\hat{m}(u)$, is given by

$$\hat{m}(u)=\arg\min_{m=0,1,...,M-1}\left(\max_{n_t=0,1,...,N_t-1}\mathrm{PAPR}\left(\{s_{u,n_t}^m(n)\}\right)\right). \quad (11)$$

In addition, it is possible to select a phase rotation sequence for the g-th stream from available B sequences, but we have confirmed by computer simulation that it achieves the same PAPR as selecting a common sequence

for all G streams from $M=B^G$ available sequences.

(b) Stream-wise frequency-domain SLM (FD-SLM)

The stream-wise FD-SLM can be depicted by Fig. 2(b). Phase rotation is applied to the frequency components $\{\mathbf{D}_u(k);k=0\sim N_c-1\}$, i.e. after DFT operation in (1). The phase-rotated frequency-domain streams corresponding to the m-th phase rotation sequence is represented by $\{\mathbf{D}_u^m(k);k=0\sim N_c-1\}$, where $\mathbf{D}_u^m(k)$ is

$$\mathbf{D}_u^m(k)=[\Phi_m(k)D_{u,0}(k),...,\Phi_m(k)D_{u,g}(k),...,\Phi_m(k)D_{u,G-1}(k)]^T. \quad (12)$$

Then, $\{\mathbf{D}_u^m(k)\}$ is passed through signal processing described in (2)-(6). The selection criterion in stream-wise FD-SLM is exactly the same as described in the stream-wise TD-SLM in (11). Note that the stream-wise FD-SLM is available for SC only since the OFDM does not require the DFT before Tx. filtering [9].

3.2. Phase rotation sequence estimation

In general, if the SLM is applied at the transmitter, the receiver needs to conduct de-mapping before data de-modulation. Assuming $\{\hat{\mathbf{D}}_u(k);\ k=0\sim N_c-1\}$ with $\hat{\mathbf{D}}_u(k)=[\hat{D}_0(k),...,\hat{D}_{G-1}(k)]^T$ and $\{\hat{\mathbf{d}}_u(n);\ n=0\sim N_c-1\}$ with $\hat{\mathbf{d}}_u(n)=[\hat{d}_{u,0}(n),...,\hat{d}_{u,G-1}(n)]^T$ are respectively the received frequency-domain component streams and the received time-domain data streams of the u-th user before de-mapping, the de-mapped signals of stream-wise FD-SLM and stream-wise TD-SLM are expressed by

$$\begin{cases}\tilde{\mathbf{D}}_u(k)=\Phi^*_{\hat{m}(u)}(k)\hat{\mathbf{D}}_u(k) & \text{for FD-SLM}\\ \tilde{\mathbf{d}}_u(n)=\Phi^*_{\hat{m}(u)}(n)\hat{\mathbf{d}}_u(n) & \text{for TD-SLM}\end{cases}. \quad (13)$$

However, (13) requires side-information transmission to know $\hat{m}(u)$. To achieve blind SLM, the receiver needs to estimate the selected phase rotation sequence. Phase rotation sequence estimation [7,9] is carried out by utilizing the fact that the received signal constellation obtained from correct de-mapping is close to the original modulation mapping. The difference between those constellations obtained from correct and incorrect de-mapping can be decided by computing Euclidean distance. Here, we assume that the estimation is carried out separately for each UE's received signal.

In the stream-wise FD-SLM, the frequency-domain received candidate corresponding to the q-th de-mapping sequence is obtained as $\{\hat{\mathbf{D}}_u^q(k)=\Phi_q^*(k)\hat{\mathbf{D}}_u(k);\ k=0\sim N_c-1\}$. Each frequency-domain stream $\{\hat{D}_{u,g}^q(k)=\Phi_q^*(k)\hat{D}_{u,g}(k);\ k=0\sim N_c-1\}$, $g=0\sim G-1$, is then transformed into time-domain received data stream $\{\hat{d}_{u,g}^q(n);\ n=0\sim N_c-1\}$, $g=0\sim G-1$, by N_c-point IDFT. The Euclidean distance between $\{\hat{d}_{u,g}^q(n)\}$ and the closet constellations is computed. The estimated phase rotation sequence of the u-th user $\{\Phi_{\tilde{m}(u)}(k)\}$, with the index $\tilde{m}(u)$, is found by

$$\tilde{m}(u)=\arg\min_{q=0,1,...,M-1}\left(\varepsilon=\sum_{g=0}^{G-1}\sum_{n=0}^{N_c-1}\left|\hat{d}_{u,g}^q(n)-c\right|^2\right), \quad (14)$$

Table 1 Simulation parameters.

User equipment	Data modulation	16QAM, 64QAM
	No. of subcarriers	N_c=128
	CP length	N_g=16
	Tx. filter	SVD w/ MMSE power allocation
	No. of Tx. antennas	N_t=2,4
	No. of streams per UE	G=N_t=2,4
SLM parameter	Phase rotation type	Random polyphase
	No. of phase sequences	M=1~512
Channel	Fading	Frequency-selective block Rayleigh
	Power delay profile	Symbol-spaced, 16-path uniform
Base station	No. of Rx. antennas	N_r=4,8
	Channel estimation	Ideal
	Rx. filter	MMSE
	Phase rotation sequence estimation method	Maximum-likelihood

where $c\in\Psi_{\text{mod}}$ is the original data-modulated constellation (i.e. QAM mapping). The estimation in (14) can be done by either exhaustive search (maximum-likelihood; ML) [7] or 2-step estimation using Viterbi algorithm [13].

In the stream-wise TD-SLM, the time-domain received candidate corresponding to the q-th de-mapping sequence is obtained as $\{\hat{\mathbf{d}}_u^q(n)=\Phi_q^*(n)\hat{\mathbf{d}}_u(n);\ n=0\sim N_c-1\}$, where $\hat{\mathbf{d}}_u^q(n)=[\hat{d}_{u,0}^q(n),...,\hat{d}_{u,G-1}^q(n)]^T=[\Phi_q^*(n)\hat{d}_{u,0}(n),...,\Phi_q^*(n)\hat{d}_{u,G-1}(n)]^T$, $g=0\sim G-1$. The estimated phase rotation sequence of the u-th user $\{\Phi_{\tilde{m}(u)}(n)\}$, with the index $\tilde{m}(u)$, is determined by substituting $\{\hat{\mathbf{d}}_u^q(n)=\Phi_q^*(n)\hat{\mathbf{d}}_u(n)\}$ in (14). Finally, the received data streams before de-modulation can be obtained by replacing $\tilde{m}(u)$ instead of $\hat{m}(u)$ in (13).

4. Performance evaluation

Simulation parameters are summarized in Table 1. Uplink MMSE-SVD consisting of U=2 UEs is assumed. Channel coding and ARMC are not considered for simplicity. Performance evaluation is done and discussed in terms of PAPR, BER and computational complexity. Performance of the proposed stream-wise SLM is also compared with that of the antenna-wise SLM with perfect $N_t\log_2(M)$-bit side-information detection [10].

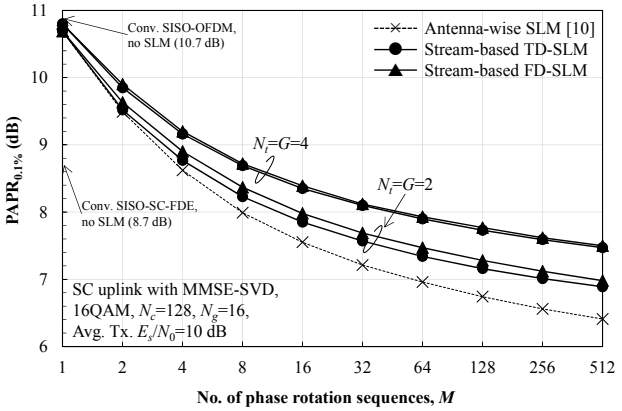

Fig. 3 $\text{PAPR}_{0.1\%}$ versus the number of candidates.

4.1. PAPR performance

PAPR performance is evaluated by measuring the PAPR value at complementary cumulative distribution function (CCDF) equals 10^{-3}, called $PAPR_{0.1\%}$. Fig. 3 shows $PAPR_{0.1\%}$ versus the number of phase rotation sequences (M) of SC-MU-MIMO uplink using SVD-MMSE filtering. The data modulation scheme is set to be 16QAM. $PAPR_{0.1\%}$ of the conventional single-antenna OFDM without SLM (10.7 dB) and the conventional single-antenna SC without SLM (8.7 dB) are also plotted for comparison. The total transmit E_s/N_0 is set to be 10 dB.

Firstly, it is seen when M=1 (no SLM) that the use of SVD filtering with joint Tx/Rx MMSE power allocation drastically increases the PAPR of SC waveform [5]. PAPR can be reduced by increasing M in both the antenna-wise SLM and the stream-wise SLM, but the PAPR of SC-MU-MIMO using the stream-wise SLM is higher than that of the antenna-wise SLM. This is because the phase rotation is carried out before Tx. filtering, which decreases the degree of freedom in waveform candidate generation [8-9]. The increasing of PAPR becomes obvious when N_t=4, where the PAPR of the antenna-wise SLM is irrespective with N_t. Assuming that N_t=2 and M=512, the stream-wise FD-SLM and the stream-wise TD-SLM can lower the PAPR by 3.7 dB and 3.8 dB, respectively, which are only 0.5 dB higher than that of the antenna-wise SLM (a.k.a. an optimal solution).

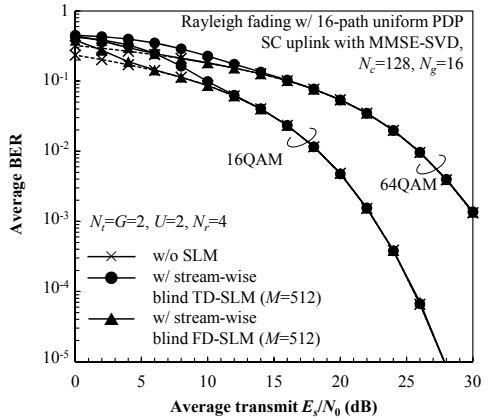

(a) $(U\times N_t,N_r)=(2\times2,4)$

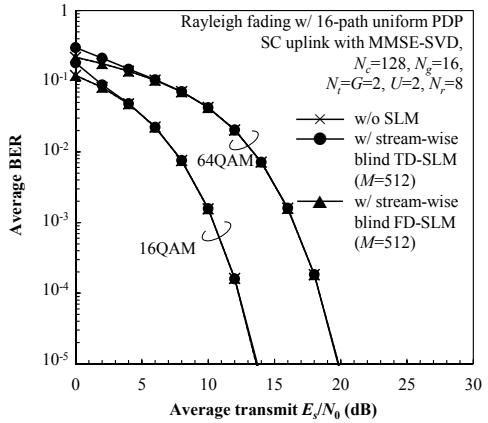

(b) $(U\times N_t,N_r)=(2\times2,8)$

Fig. 4 BER performances.

It is also seen that there is no major difference in PAPR performances of TD-SLM and FD-SLM when considering uplink MMSE-SVD filtering, which is inconsistent with single-antenna transmission case [7]. This is because the output signals after applying the Tx. filtering are not the original or the phase-rotated version of data-modulated symbols and hence, the advantage of smaller subspace for searching the low-PAPR waveform in TD-SLM becomes unavailable. In addition, we have also evaluated the PAPR of SC-MU-MIMO with MMSE-SVE filtering using 64QAM, but the results are not shown in this paper since they are very similar to those of 16QAM.

4.2. BER performance

Figs. 4(a) and 4(b) show the uncoded average BER of uplink MMSE-SVD and the stream-wise blind SLM as a function of average total transmit E_s/N_0 when the MU-MIMO system configurations $(U\times N_t,N_r)$ equal (2×2,4) and (2×2,8), respectively. BER of the uplink MMSE-SVD without SLM [4] is also plotted for comparison. The number of phase rotation sequences is M=512. In addition, performance comparison of uplink MMSE-SVD and receive ZF has been examined in [4], hence the BER of SC-MU-MIMO with ZF filtering is not discussed here.

It is seen from Fig. 4 that there is no major difference among BER performances of transmission without SLM, transmission with stream-wise blind FD-SLM and with stream-wise blind TD-SLM although there is no side-information sharing, especially when the average transmit E_s/N_0 is sufficiently high. The stream-wise blind FD-SLM can keep the BER performance very close to that of transmission without SLM even in low-E_s/N_0 region. This is consistent with [9] since the difference between the received signal obtained from correct de-mapping and incorrect de-mapping in blind FD-SLM is more obvious than that of blind TD-SLM, resulting in higher accuracy in phase rotation sequence estimation.

In addition, the BER degradation at low-E_s/N_0 region is improved when N_r increases from 4 to 8 because an increasing in N_r results in higher spatial diversity gain and simultaneously mitigates the effects of fading and noise. As a consequent, the accuracy of phase rotation sequence estimation in (14) is improved.

4.3. Computational complexity

Computational complexity is evaluated by counting the number of complex-valued multiplication operations [14]. For simplicity, we consider the complexity of SLM algorithm at the transmitter and the complexity of phase rotation sequence estimation at the receiver only. The computational complexity is determined by Table 2. Note that the complexity of 2-step Viterbi estimation is calculated based on 27-state trellis diagram

It is difficult to discuss the computational complexity comparison by using Table 2 only, hence we calculate the number of complex-valued multiplication operations assuming N_c=128, M=512, N_t=G=2, N_r=4 and V=8 as an

example. The computational complexity of antenna-wise SLM algorithm, stream-wise FD-SLM and stream-wise TD-SLM are 1.16×10^7, 1.17×10^7 and 1.27×10^6, respectively (these numbers can be depicted as 260 times of SVD operation [13]). The complexity of stream-wise FD-SLM is higher than that of antenna-wise SLM by only 1%, and by 10% for the stream-wise TD-SLM.

Meanwhile, phase rotation sequence estimation of the antenna-wise SLM has not been determined and is expected to be impractical since it needs to generate the received symbol replica based on all possible Rx. filter coefficients. The use of stream-wise blind FD-SLM is attractive in terms of BER performance (see Fig. 4), but the phase rotation sequence estimation of blind FD-SLM requires higher computational complexity than that of blind TD-SLM, e.g. about 8 times higher when N_c=128. The complexity of phase rotation sequence estimation of stream-wise blind TD-SLM can be further reduced by using the 2-step Viterbi estimation, where its reduction capability becomes obvious when M>128 [13].

Based on the computer simulation results in Sects. 4.1-4.3, the stream-wise blind FD-SLM is recommended for keeping the BER very close to the transmission without SLM but at the cost of high computational complexity at the receiver. On the other hand, the stream-wise blind TD-SLM is recommended for keeping the receiver structure simple but at the cost of BER degradation at the low-E_s/N_0 region.

5. Conclusion

Two stream-wise blind SLM schemes for uplink MMSE-SVD were introduced in this paper. The sub-optimal blind SLM employs phase rotation sequence multiplication to transmit data streams, either in time domain (i.e. blind TD-SLM) or in frequency domain (i.e. blind FD-SLM), and prior to SVD filtering. The phase rotation sequence estimation for stream-wise blind SLM can be carried out similar to that of single-antenna blind SLM [7,13]. Computer simulation results confirmed that the stream-wise blind SLM can lower the PAPR of SC-MU-MIMO signal by 3.8 dB when M=512 and N_t=2, which is only 0.5 dB apart from the optimal value. It is also shown that no significant BER degradation occurs even though there is no side-information transmission.

In addition, the stream-wise blind SLM techniques also can be applied to the downlink MMSE-SVD without major changes on both the filter implements and SLM algorithms. Performance evaluation of the stream-wise blind SLM for downlink MMSE-SVD is left as our future works.

Acknowledgement

This paper includes a part of results of "The research and development project for realization of the fifth-generation mobile communications system" commissioned to Tohoku University by The Ministry of Internal Affairs and Communications (MIC), Japan.

Table 2 Computational complexity (per UE).

		Antenna-wise SLM	Stream-wise FD-SLM	Stream-wise TD-SLM
SLM algorithm		$M\times N_t\times$ $(VN_c\log_2 VN_c$ $+N_c+VN_c)$	$M\times N_t\times$ $(VN_c\log_2 VN_c+1$ $+(G+V)N_c)$	$M\times N_t\times$ $(VN_c\log_2 VN_c+1$ $+(G+V)N_c$ $+N_c\log_2 N_c)$
Phase sequence estimation	**ML**	N/A	$M\times N_t\times N_c\times$ $(\log_2 N_c+1)$	$M\times N_t\times N_c$
	2-step Viterbi		N/A	N_{trellis} $\le 81\times(N_c-2)$

References

[1] 5GMF White Paper, *5G Mobile Communications Systems for 2020 and beyond*, Ver. 1.01, Jul. 2016.

[2] H. G. Myung, J. Lim and D. J. Goodman, "Single Carrier FDMA for Uplink Wireless Transmission," *IEEE Veh. Technol. Mag.*, Vol. 1, No. 3, pp. 30-38, Sept. 2006.

[3] D. Gesbert, M. Kountouris, R. W. Heath Jr., C. B. Chae and T. Salzer, "Shifting the MIMO Paradigm," *IEEE Signal Process. Mag.*, Vol. 24, No. 5, pp. 36-46, Oct. 2007.

[4] S. Kumagai and F. Adachi, "Joint Tx/Rx MMSE Filtering for Single-Carrier MU-MIMO Uplink," *Proc. IEEE VTS Asia Pacific Wireless Commun. Symp. (APWCS2015)*, Singapore, Aug. 2015.

[5] S. Kumagai, T. Obara, T. Yamamoto and F. Adachi, "Joint Tx/Rx MMSE Filtering for Single-Carrier MIMO Transmission," *IEICE Trans. Commun.*, Vol. E97-B, No. 9, pp. 1967-1976, Sept. 2014.

[6] R. W. Bauml, R. F. H. Fischer and J. B. Huber, "Reducing the Peak-to-Average Power Ratio of Multicarrier Modulation by Selected Mapping," *IEEE Electron. Lett.*, Vol. 32, No. 22, pp. 2056-2057, Oct. 1996.

[7] A. Boonkajay and F. Adachi, "A Blind Polyphase Time-Domain Selected Mapping for Filtered Single-Carrier Signal Transmission," *Proc. IEEE Veh. Technol. Conf. (VTC2016-Fall)*, Montréal, Canada, Sept. 2016.

[8] A. Boonkajay and F. Adachi, "Blind Selected Mapping Technique for Space-Time Block Coded Transmit Diversity with Transmit Frequency-Domain Equalization," *IEICE Tech. Rep.*, Vol. 116, No. 479, RCS2016-290, pp. 7-12, Mar. 2017.

[9] F. Adachi, A. Boonkajay, Y. Seki. T. Saito, S. Kumagai and H. Miyazaki, "Cooperative Distributed Antenna Transmission for 5G Mobile Communications Network," *IEICE Trans. Commun.*, Vol. E100-B, No. 8, Aug. 2017.

[10] M. S. Baek, M. J. Kim, Y. H. You and H. K. Song, "Semi-Blind Channel Estimation and PAR Reduction for MIMO-OFDM System with Multiple Antennas," *IEEE Trans. Broadcast.*, Vol. 50, Issue 4, pp. 414-424, Dec. 2004.

[11] R. F. H. Fischer and M. Hoch, "Directed Selected Mapping for Peak-to-Average Power Ratio Reduction in MIMO OFDM," *IEE Electron. Lett.*, Vol. 42, No. 22, pp. 1289-1290, Oct. 2006.

[12] C. Seigl and R. F. H. Fischer, "Transmission and Detection of Side Information for Selected Mapping in MIMO OFDM," *Proc. Int. ITG Workshop on Smart Antennas (WSA 2010)*, Bremen, Germany, Mar. 2010.

[13] A. Boonkajay and F. Adachi, "2-Step Signal Detection for Blind Time-Domain Selected Mapping," *IEICE Tech. Rep.*, Vol. 116, No. 257, RCS2016-182, pp. 161-166, Oct. 2016.

[14] G. H. Golub and C. F. van Loan, *Matrix Computations*, 3rd-ed., Johns Hopkins Univ. Press, 1996.